UWB Device for Microwave Imaging: Validation through Phantoms

Alessandro Vispa[1], Lorenzo Sani[1], Martina Paoli[1], Alessandra Bigotti[1], Giovanni Raspa[1] , Navid Ghavami[1], Mohammad Ghavami[2], Gianluigi Tiberi[1,2]

[1] UBT - Umbria Bioengineering Technologies, Spin off of University of Perugia, Perugia, Italy,
[2] School of Engineering, London South Bank University, London, UK,
alessandro.vispa@gmail.com, gianluigi@ubt-tech.com

***Abstract*— Breast cancer detection is still a challenging subject, and this has forced physical, chemical and engineering research to explore new detection modalities. In this context, microwave imaging has received increasing attention in the last decades. Such effort has been encouraged by the fact that, at microwave frequencies, it is possible to distinguish between tissues with different dielectric constant values. In such framework, an innovative microwave instrument is presented here. The apparatus, consisting of 2 antennas operating in air, is completely safe and non-invasive since it does not emit any ionizing radiation and it does not require any breast crushing. We use Huygens Principle to provide fresh understanding into breast cancer detection. The algorithm based on this principle provides inhomogeneity maps of the dielectric properties (dielectric constant and/or conductivity) of different tissues, highlighting their contrast in the resulting final image. The experimental results on phantoms with different dielectric constants and inclusions are presented here. Moreover, on the basis of this analysis, we establish a modality to detect the presence of inclusions inside phantoms.**

***Index Terms*—Antenna, Propagation, Measurement.**

I. INTRODUCTION

Breast cancer (BC) is the most prevalent form of cancer in women. One in nine women will acquire BC at some point in their life and one in thirty will die from the disease [1-2].

To achieve early diagnosis, in the last two decades, a new imaging technique based on microwave radiation has been developed [3-8]. Nowadays microwave imaging (MI) is being accepted as an attainable option or complementary technique to the consolidated classical methods such as mammography, magnetic resonance imaging (MRI) or ultra-sound imaging. MI introduces some advantages with respect to the conventional examinations. First of all MI is free from ionizing radiations (X-rays), which are not recommended for screening purposes in women under the age of 50 [9-10]. Moreover, during the examinations carried out with MI, the patient appears to be more comfortable since this type of measurement does not require the painful compression of the breast. The physical principle of the MI techniques lies in a different perspective of the breast; in fact, rather than the density, microwaves respond differently if they hit tissues having different dielectric properties, A significant contrast between healthy breast tissue and malignant tissue is present at microwave frequencies; this contrast is shown to be up to a factor of 5 in conductivity and permittivity. Meanwhile, newer studies suggest the existence of this contrast only between fatty and malignant breast tissues, and a lower contrast (as low as 10% in dielectric properties) between healthy fibro glandular and malignant tissues [11-14].

At present, some MI prototypes for breast cancer detection are at clinical trials stage [15, 16]. Recently, a novel microwave apparatus (MammoWave, UBT Srl, Perugia, IT) started clinical validation [17]. In MammoWave, microwave signals are processed through Huygens principle (HP) [18]. The methodology allows to differentiate between different tissues, or different conditions of tissues, and to get a final image, which represents a homogeneity map of the dielectric properties (dielectric constant and/or conductivity). Ultra wideband (UWB) technology permits the use of all the information in the frequency domain by combining the information of the individual frequencies to build such image. The HP method can identify the presence and the position of significant dispersions, i.e. inclusions within a volume.

In this paper, we will present a brief description of MammoWave and we will present some results achieved through phantom validations.

II. THEORETHICAL FRAMEWORK

In accordance with the HP, each element of a wave front can be considered as a secondary source of spherical waves in phase and with amplitude proportional to the primary wave. It is therefore possible to determine the perturbation produced at any point in space by the overlap of all secondary waves that reach such a point. From an operational point of view, the signal received by the receiver antenna (RX) is the field generated by the overlap of *N*

points along the circumference and reconstructed through the HP. The final intensity of the image will depend on the superimposed fields, which are functions of the frequencies and relative positions between transmission (TX) and reception (RX).

Let us consider the system described in Fig. 1. A cylinder (striped black circle) illuminated by a transmitting source tx_m that operates in a given frequency band. We assume that the dielectric properties of the cylinder, i.e. the dielectric constant ε_r and the conductivity σ, are known. The cylinder contains an inclusion (grey circle in Fig. 1), here assumed to be cylindrically shaped and with a different dielectric constant and/or conductivity. The problem consists of identifying the presence and location of the inclusion by using only the field measured outside the cylinder [18-19].

The external cylinder is illuminated using a range of different frequencies and from different illuminating points; all the reconstructed fields will exhibit the mismatch, which will always be located in the region of transition of the two media. It should be noted that we are not interested in evaluating the internal field, but rather to verify if HP can determine the contrast and locate an inclusion within a volume. It follows that the reconstructed field will show a discrepancy in the transition region between two different media. The approach allows using all the information in the frequency domain, thus by summing incoherently all the information of the single frequencies, that is, the reconstructed fields, the inclusion will be detected and localized.

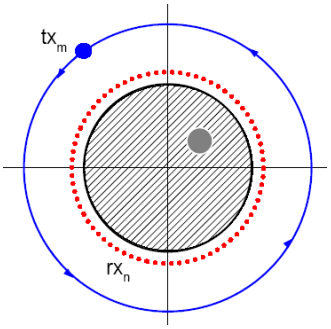

Fig. 1: (color online). Schematic illustration of a section of the system. Transmitting (light blue line) and receiving positions (red dots) containing the sample (black line) are shown. A section of the inclusion (grey circle) is shown inside the receiving circle.

Fig. 2: MamoWave Device installed at the Breast Unit, Department of Diagnostic Imaging, Foligno Hospital, Italy. Clinical trials are ongoing under a protocol approved by the Ethical Committee of Regione Umbria, Italy (N. 6845/15/AV/DM of 14/10/2015, N. 10352/17/NCAV of 16/03/2017).

III. Materials and Methods

All microwave phantoms' images and all the results shown in this paper were reconstructed from data gathered using the apparatus MammoWave installed at the Department of Diagnostic Imaging, Foligno Hospital, Foligno, Italy. The device, shown in Fig. 2, consists of two antennas operating in air. The antennas are connected to a Vector Network Analyzer (VNA).

The TX and RX antennas are placed at the same height and can be moved on the azimuthal plane, to irradiate (TX) and subsequently receive (RX) the microwave signals. The TX plane is divided into 5 sections of 72°. In each section the transmitting antenna occupies the zero position of the section (0°, 72°, 144°, 216°, 288°) plus two other separate positions of 4.5° from each other. These form a triplet within each section. The RX antenna moves circularly acquiring every 4.5° (80 points).

Considering the 15 emission positions of TX, the 80 receiving positions of RX and the emitted frequencies in the range 1-9 GHz with a 5 MHz step, we get a 1200x1601 raw data matrix of S_{21} values.

The device's internal surfaces were shielded with absorber material to create an anechoic chamber. The instrument (appropriately integrated with a bed) is additionally constituted by: a hub with a cup that are placed to contain the breast of the patient (prone positioned) or the container of samples and two arms to associate TX and RX to the hub through rotation.

The capability of the instrument to detect and localize an inclusion has been verified through measurements in phantoms. In this context, a PMMA cylinder with 11 cm diameter and 23 cm height has been used as a container for the liquid under examination. The samples taken into consideration have been oil and glycol. To reproduce the inclusions tubes of 1, 5 and 10 mm diameter filled with distilled water or glycol have been used. In more details, the following measurements have been carried out:

i) Homogeneous sample consisting of oil.
ii) Homogeneous sample consisting of glycol.
iii) Homogeneous sample consisting of oil with glycol inclusion.
iv) Homogeneous sample consisting of oil with water inclusion.
v) Homogeneous sample consisting of glycol with water inclusion.

The acquired matrices have been analyzed with a dedicated software that allows the reconstruction of an image. Details on the reconstruction algorithm can be found in [18, 19]. The analysis of the image allows to obtain some parameters, among which is the ratio between maximum and average of the image intensity (MAX/AVG).

IV. Results

In this paper we show the results which correspond to the homogeneous sample of oil, and oil with glycol inclusion with 10 mm diameter. As shown by comparing Figs. 3a and

3b, the contrast due to the difference in dielectric properties between oil and glycol is highlighted by an increase in intensity in the region where the test tube was placed.

We also compared the MAX/AVG values. Specifically, MAX/AVG of the image corresponding to homogeneous sample of oil has a MAX/AVG equal to 1.42. Conversely, MAX/AVG of the image corresponding to homogeneous sample of oil with glycol inclusion has a MAX/AVG equal to 1.95. It is evident that the presence of the inclusion, and therefore a variation of dielectric constant between the two materials, leads to a separation (quantified through MAX/AVG) between the values relative to the homogeneous sample and the values relative to the sample with a test tube.

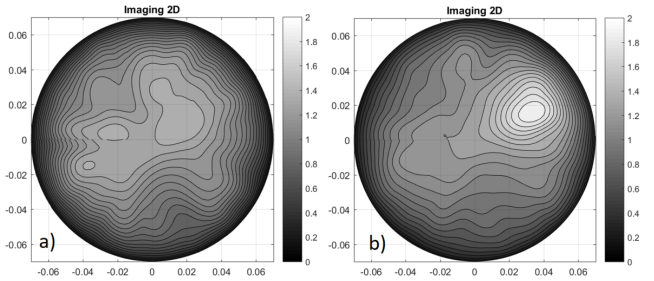

Fig. 3: Images resulting from the analysis. Black and white maps show the dielectrics inhomogeneities (in arbitrary units) reconstructed by Huygens Principle. In order to compare different samples, images have been normalized to the average value to have the same intensity scales. (a) Image relative to the homogeneous oil sample. (b) Image of oil sample having glycol test tube: the white spot highlights the presence of the inclusion. Axis units are in meters [m],

To confirm the localization of the peak and therefore of the inclusion, a series of measurements have been carried out by rotating the test tube each time with a step of 45 degrees. The positioning has been performed through a goniometric ring placed around the housing of the sample holder container. Fig. 4 shows the resulting images obtained rotating the inclusion. Peak detection ensures the location of the inclusion in all configurations.

Moreover, since the acquisition is performed in the frequency range between 1 and 9 GHz, it is possible to view the individual frequency contributions. This allows to determine the correlation between the dielectric response and the individual frequency range. As shown in the Fig. 5, in this case, the presence and location of the inclusion is visible at all frequencies, although the characteristics of the peak varies with the frequency itself. Taking into account the values of MAX/AVG (Fig. 6), an increase in this parameter is evident with the increase in frequency. This trend is due to the better definition of the peak, which consequently decreases the average value in the intensity of the image.

V. CONCLUSIONS

A new microwave imaging device based on the Huygens principle has been analyzed and validated through phantom measurements. Using this procedure, it is possible to observe the contrast, which is the variation of the dielectric properties of the materials under investigation.

The device allows achieving all the information in the frequency domain to be used by combining the single frequency information to construct an image. The procedure is robust and permits, in the presence of a contrast, the detection and localization of inclusions within the volume. Validation of the device through experiments has been performed and presented, illustrating its effectiveness. It has been shown that MAX/AVG of phantom with inclusion is >30% than MAX/AVG of phantom without inclusion.

It is worthwhile to underline that the measurement data contains noise. Although the presence of noise does not affect detection and localization, research is underway on both hardware and software to improve the signal-to-noise ratio.

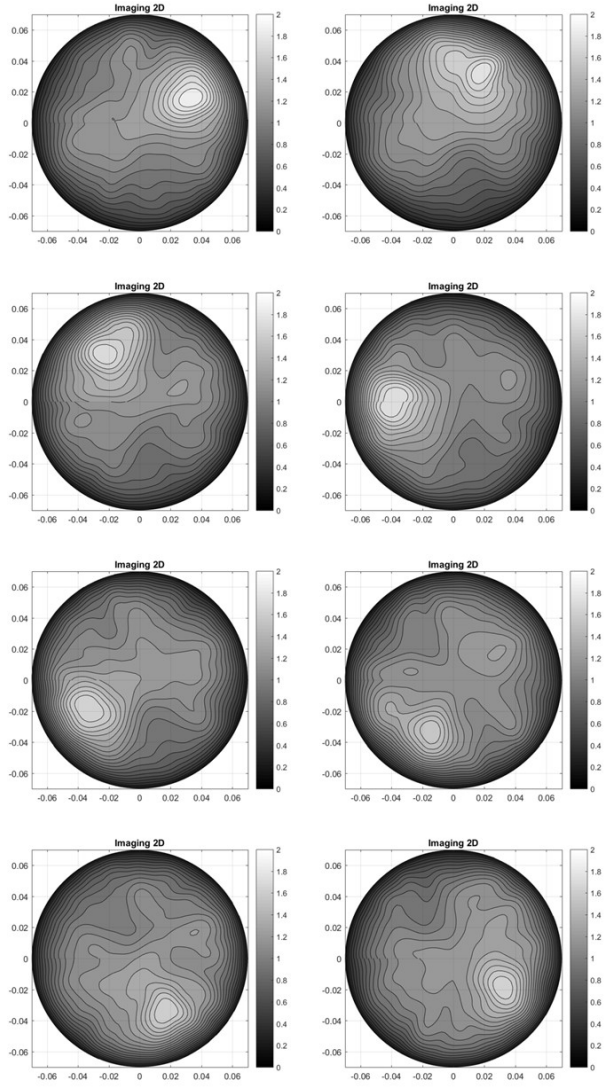

Fig. 4: Images obtained by 45° rotation of the test tube inside the oil sample. For all configurations, the peak is clearly visible, guaranteeing the proper functioning of the instrument and of the analysis method. Axis are in meters [m]. Intensity map show the dielectrics inhomogeneities (in arbitrary units) reconstructed by Huygens Principle.

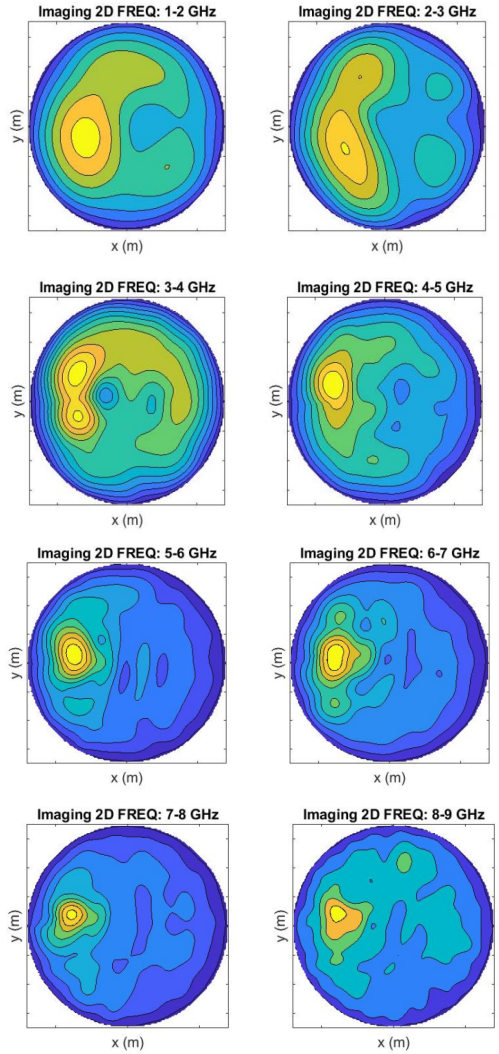

Fig. 5: Images of the test tube inside the oil sample for different frequency bands. All the images have been normalized to the correspondent maximum. The presence of a peak related to the inclusion of glycol is evident, for all the frequency range scanned. Axis are in meters [m].

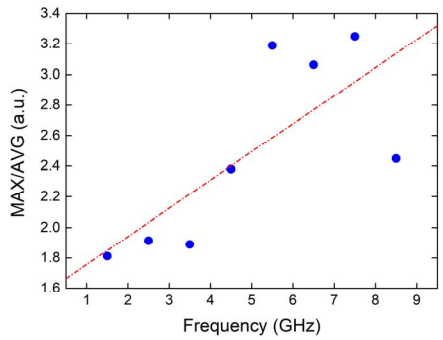

Fig. 6. The ratio between the values of maximum and the average (blue circles) increases with frequency. Red line is obtained through linear fitting.

ACKNOWLEDGMENT

This project has received funding from the European Union's Horizon 2020 research and innovation programme under grant agreement No 830265.

REFERENCES

[1] OECD (2017), Health at a Glance 2017: OECD Indicators, OECD Publishing, Paris.

[2] D.M. Parkin, F. Bra, J. Ferlay, P. Pisani, "Estimating the world cancer burden". Globocan 2000. Int J Cancer, 94 153156 (2001).

[3] N.K. Nikolova, "Microwave Imaging for Breast Cancer", IEEE Microwave Magazine 12 (7) 78-94 (2011).

[4] E.C. Fear, P.M. Meaney, M.A. Stuchly, "Microwaves for breast cancer detection?", IEEE Potentials, 22 (1) 12-18 (2003).

[5] P.M. Meaney, K.D. Paulsen, "Nonactive antenna compensation for fixed-array microwave imaging: Part II imaging results," IEEE Trans. Med. Imag. 18 (6)508518 (1999).

[6] D.W. Winters, B.D. Van Veen, S.C. Hagness, "A sparsity regularization approach to the electromagnetic inverse scattering problem," IEEE Trans. Antennas Propag. 58 (1) 145154 (2010).

[7] M. Chiappe, G.L. Gragnani, "An analytical approach to the reconstruction of the radiating currents in inverse electromagnetic scattering," Microw. Opt. Technol. Lett. 49 (2) 354360 (2007).

[8] G.L. Gragnani, "Two-dimensional non-radiating currents for imaging sys-tems: theoretical development and preliminary assessment," IET Microw. Antennas Propag. 3 (8) 11641171 (2009).

[9] D.L. Miglioretti, J. Lange, J.J. van den Broek, C.I. Lee, N.T. van Ravesteyn, D. Ritley, et al, "Radiation-Induced Breast Cancer Incidence and Mortality From Digital Mammography Screening: A Modeling Study," Ann Intern Med., 164 pp. 205-214. 2016).

[10] M.S. Fuller, C.I. Lee, J.G. Elmore, "Breast Cancer Screening: An Evidence-Based Update," The Medical clinics of North America, 99(3) 451-468 (2015).

[11] S. Chaudhary, R. Mishra, A. Swarup, J.M. Thomas, "Dielectric properties of normal and malignant human breast tissues at radiowave and microwave frequencies," Indian journal of biochemistry and biophysics vol. 21 pp. 76-79 (1984).

[12] J.W. Choi, J. Cho, Y. Lee, J. Yim, B. Kang, K.K. Oh, W.H. Jung, H.J. Kim, C. Cheon, H.D. Lee, et al, "Microwave detection of metastasized breast cancer cells in the lymph node; potential application for sentinel lymphadenectomy," Breast Cancer Research and Treatment 86 (2) 107-115 (2004).

[13] M. Lazebnik, L. McCartney, D. Popovic, C.B. Watkins, M.J. Lindstrom, J. Harter, S. Sewall, A. Magliocco, J.H. Booske, M. Okoniewski , et al (2007a), "A large-scale study of the ultrawideband microwave dielectric properties of normal breast tissue obtained from reduction surgeries", Physics in medicine and biology 52(10):2637.

[14] M. Lazebnik, D. Popovic, L. McCartney, C.B. Watkins, M.J. Lindstrom, J. Harter, S. Sewall, T. Ogilvie, A. Magliocco, T.M. Breslin et al (2007b), "A large-scale study of the ultrawideband microwave dielectric properties of normal, benign and malignant breast tissues obtained from cancer surgeries", Physics in Medicine and Biology 52(20):6093.

[15] P.M. Meaney, M.W. Fanning, T. Raynolds, et al. "Initial Clinical Experience with Microwave Breast Imaging in Women with Normal Mammography", Acad Radiol 14 (2) 207-218 (2007).

[16] D. Byrne, I.J. Craddock. "Time-Domain Wideband Adaptive Beamforming for Radar Breast Imaging", IEEE Transactions on Antennas and Propagation 63 (4) 1725-1735 (2015).

[17] L. Sani, et al., "Initial Clinical Validation of a Novel Microwave Apparatus for Testing Breast Integrity," IEEE International Conference on Imaging Systems and Techniques (IST) 278-282 (2016).

[18] G. Tiberi, R. Raspa. Apparatus for testing the integrity of mammary tissues. Patent n.0001413526.

[19] G. Tiberi, N. Ghavami, D.J. Edwards, A. Monorchio, "Ultrawideband microwave imaging of cylindrical objects with inclusions," IET Microwaves, Antennas Propagation, 5 (12) (2011).

[20] N. Ghavami, G. Tiberi, D.J. Edwards, A. Monorchio, "UWB Microwave Imaging of Objects With Canonical Shape," IEEE Transactions on Antennas and Propagation 60 (1) (2012).